Journal of Information Systems Engineering and Management
2025, 10(47s)
e-ISSN: 2468-4376
https://www.jisem-journal.com/

Research Article

Improve the Properties of Flattened Dispersion Porous Core Photonic-Crystal Fiber for Terahertz Transmission

Mohammed Rafea Azeez Alobaidy[1], Marwan Hafeedh Younus[2]
12Physics department, college of education for pureb science, mosul university,Iraq
** Corresponding Author: mohammed.23esp16@student.uomosul.edu.iq*

ARTICLE INFO

Received: 31 Dec 2024

Revised: 20 Feb 2025

Accepted: 28 Feb 2025

ABSTRACT

In this paper, a solid core photonic crystal fiber (SC-PCF) for dispersion improvement and birefringence enhancement in the terahertz frequency range is proposed. The suggested SC-PCF structure contains three hexagonal layers of circular air holes in the cladding, which promises to yield very large birefringence and flat dispersion. Assuming TOPAS as the background material, the COMSOL software multiphysics 6.1, which is based on the finite element method, was used to investigate its properties. The results show that over a frequency range of 0.7–1.3 THz, the SC-PCF has negative and flat dispersion of -43.2959 Ps/THz/cm, a high birefringence of 3.7×10^{-3}, and a high power fraction of 51% with a size of circular porosity of 28%. These findings suggest that the SC-PCF could be highly effective for applications in optical communication and sensing technologies. Further research will focus on optimizing the structure to enhance its performance across different wavelengths and operational conditions. Critical parameters such as confinement loss and v parameters are also discussed in detail. So, the designed SC-PCF can be useful for polarization-maintaining applications.

Keywords: *Photonic crystal fiber; Terahertz wavelengths; Dispersion; Absorption loss; Effective area.*

INTRODUCTION

(THz) radiation or waves, with a frequency range of 0.1 to 10 THz, are situated between the microwave and infrared bands (Chen *et al.*, 2000; Liu *et al.*, 2007), have attracted the attention of researchers due to their wide applications security – sensitivity, medical imaging, and sinsing (Younus *et al.*,2021; Pawar *et al.*, 2013) and spectroscopy (Rabih *et al.*, 2201). At present, imaging (Zhang *et al.,* 2023; Yu *et al.,* 2012), sensing (Younus et al., 2017), Communications (Nagatsuma *et al.,* 2016), astronomy (Gallozzi *et al.,* 2020), and biomedical engineering for diagnosis and detection (Zaytsev *et al.,* 2015) largely rely on terahertz guided waves. This will further boost the research interest in compressed terahertz guided waves with higher refraction, ultra-flat dispersion, and low loss (Xu *et al.,* 2020; Al-Saqa *et al.,* 2023). In particular, many novel properties in ultrafast optics can be exploited by exploring the exotic dispersive properties of terahertz waveforms (Li et al., 2012). Many devices, such as optical delay lines and dispersion compensators, have been developed to generate short pulses. Recently, different types of guiders have been proposed, such as metal wire (Wang and Mittleman., 2004), metal-insulated tube (Bowden *et al.,* 2007), plastic fiber (Chen *et al.,* 2006), polymeric Bragg fiber (Skorobogatiy and Dupuis., 2007), polystyrene foam (Zhao *et al.,* 2002), hollow fiber (Hossain and Namihira., 2014), and solid fiber (Alobaidy and Younus., 2025).

All of these fibers are problematic, though, because of their strong connection to the environment, increased material loss, high bending loss, and undesired narrow band operation. As a result, photonic crystal fibers with porous cores have garnered attention lately (Chowdhury *et al.,* 2017), where design can control guide characteristics like frequency, air hole radius, air filling ratio, and core diameter. Furthermore, by choosing the right geometric parameters, low confinement loss, low dispersion anisotropy, high birefringence, and high core energy fraction in PCF can all result in low effective material loss (EML) (Chen et al., 2013). For example, a novel fiber with a honeycomb-like shell structure and a slotted hexagonal core is proposed (Islam *et al.,* 2020), which has a high birefringence, low containment loss, and low effective material loss. Further, a circular waveguide with a

Journal of Information Systems Engineering and Management
2025, 10(47s)
e-ISSN: 2468-4376
https://www.jisem-journal.com/

Research Article

porous core has been proposed at THz frequency, which achieved an extremely high birefringence and low dispersion value (Hasan *et al.,* 2016; Islam *et al.,* 2016). Recently, low material loss PCF based on TOPAS is proposed, which has low material loss at THz (Paul and Ahmed., 2019). However, because of the great qualities of the suggested guides, it has been discovered that significant confinement loss and high dispersion or birefringence can limit the terahertz transmission efficiency. As a result, PCF has a lot of room to improve in terms of dispersion and loss parameter optimization. In this study, we suggested two varieties of porous core PCF, with hexagonal circular air holes in the shell and asymmetric circulre/square air holes in the core. The objective is to flatten the dispersion and minimize the loss. Under the adjusted structural parameters, several crucial optical characteristics of the suggested PCF are also covered, including effective mode area, core photonic crystal fiber in cross-section.

energy fraction, and active material loss (EML). The primary benefit of the suggested PCF is its straightforward structure, which will enable manufacture utilizing current manufacturing processes such in situ polymerization, gel casting, and 3D printing.

DESINING PROPOSED SC-PCF

The air-filling fraction of the external structure used determines the optical properties of photonic crystal fibers. This includes geometric features like the diameter of the air holes and the distance between successive air holes. Additionally, the hexagonal shape was chosen in order to maintain the proposed SC-PCF compact, which could result in better light confinement. A Topas (n = 1.53) is used to create the hexagonal cladding with a core, as depicted in Figure 1. The three layers of cladding used in the basic SC-PCF design comprised thirty-six hexagon-shaped air holes. Each of the 36 air holes has the same dimension (D) and pitch size(ʌ), which is the separation between two successive air holes.

The air hole diameters of the layers for the SC-PCF design were chosen for this investigation to be about 200 µm, 220 µm, and 240 µm. The υ of 350 µm and the core diameter of 300 µm were chosen. Inside the fiber core, two tiny air holes of varying dimensions and shapes (circle and squre) were placed as porosity. Small air holes with widths of 20 µm, 30 µm, and 40 µm were chosen to provide porosity of 7%, 16%, and 28%, respectively. Additionally, by reducing the amount of material in the core, adding tiny air holes helps lower the fiber's overall production costs.

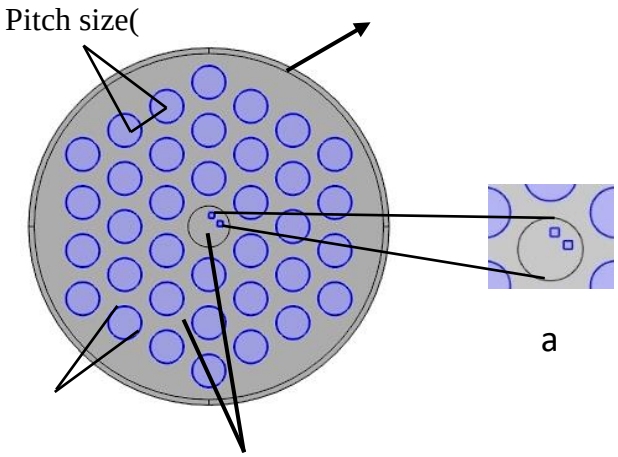

figure 1: Diagram showing the hexagonal

NUMERICAL CHARACTERIZATIONS

In order to describe the proposed waveguide, it is necessary to analyze many important optical characteristics with respect to different geometric changes. The fiber specifications for future manufacturing will be improved as a

Journal of Information Systems Engineering and Management
2025, 10(47s)
e-ISSN: 2468-4376
https://www.jisem-journal.com/

Research Article

result. Effective material loss (EML), confinement loss, core power percentage, single-mode cutoff frequency, and dispersion are the main characteristics being studied.

DISPRESION

There are two types of optical sources: monochromatic and polychromatic. Since speed is frequency dependant, the propagation delay between various transmitted light frequencies causes the spreading of sent pulses, also referred to as modal dispersion. To enable long-distance transmission, dispersion—an unfavorable factor—must be reduced or compensated for. The following equation (Haque *et al.,* 2015) can be used to examine this modal dispersion.

$$\beta_2 = \frac{2}{c}\frac{dn_{eff}}{d\omega} + \frac{\omega}{c}\frac{d^2 n_{eff}}{d\omega^2}\ ps/\ THz/\ cm \qquad (1)$$

n_{eff} and c: Effective refractive index and velocity in free space respectively, ω=2πf representing the angular frequency. The distribution of pulses per unit frequency across a given transmission distance is used to quantify dispersion. The dispersion profile of a PC-PCF must permit the transmission of pulses with minimal pulse broadening across a wide frequency band. Terahertz sensing and filtering applications require low-dispersion PC-PCFs (Aljunid et al., 2016).

Sellmeyer equation this used to analyze the material dispersion in the topaz-based wave guide and the geometric index model for solid core photonic crystal fibers (SC-PCF) is used to estimate the wave guide dispersion (Brückner, 2011). The material dispersion must match the waveguide dispersion in order to determine the zero-dispersion point, where D(λ)=0. The waveguide dispersion must have the same magnitude as the material dispersion but the opposite sign, i.e., Dw(λ) = -Dm(λ). This can be achieved by choosing appropriate structural features.

CONFENEMENT LOSS

The movement of light energy from the core into the cladding is referred to as confinement loss. This unfavorable parameter, which is determined by the following equation, needs to be decreased (Haque *et al.,* 2015).

$$L_c = 8.686 \times K_0 \times Im(neff) dB\ /\ m \qquad (2)$$

$Im_{(neff)}$: The effective refractive index's imaginary component is represented by $Im_{(neff)}$, while the free-space wavenumber is indicated by $K_o = 2\pi/\lambda$.

EFFECTIVE AREA (Aeff)

In optical fibers, A_{eff} denotes the area that the electic filed (E-field)" is dispersed throughout. It measures the fiber's power capacity or light intensity while reducing nonlinear effects. In terms of numerical aperture, nonlinearity, leakage loss, and significant bending losses, the effective area is a crucial parameter for evaluating nonlinear phase shifts (Chou Chau et al., 2015). The following equation (Haque et al., 2015) can be used to illustrate this:

$$A_{eff} = \frac{(\int\int_{-\infty}^{+\infty} |E|^2 dxdy)^2}{\int\int_{-\infty}^{+\infty} |E|^4 dxdy} \qquad (3)$$

A_{eff} : Effective area, E: Electric field.

A_{eff}. Varies with different fibers the outcome is depending upon the refractive index distribution of the fiber in the operational wavelength

EFFECTIVE MATERIAL LOSS (α_{EML})

When examining the power distribution mode in the core of photonic crystal fibers (PCF), this parameter is essential.

The following formula (Sultana et al., 2018) can be used to compute the inverse relationship between effective material loss and power distribution for PCFs:

$$\alpha_{EML} = \frac{1}{2}\sqrt{\frac{\varepsilon_0}{\mu_0}}\left(\frac{\int_{mat} n_{mat}|E|^2 \alpha_{mat} dA}{\int_{All} S_z dA}\right) \qquad (4)$$

Journal of Information Systems Engineering and Management
2025, 10(47s)
e-ISSN: 2468-4376
https://www.jisem-journal.com/

Research Article

α_{EML} : Effective material loss, α_{mat} : Material absorption loss of Topas, A: Area of the Topas material, E: Electric field component corresponding to that region, ε_o and μ_o : Permittivity and permeability of free space respectively, and S_z :Z-component the pointing vector. n_{mat}; material refractive index. The whole area of the mode is shown by the denominator in the previously described equation, which is(i.e., $\int_{all}$, S_z dA).

POWER FRACTION

The power fraction, which represents the amount of usable power transmitted through the fiber's core, is another crucial factor for evaluating the performance of photonic crystal fibers with a crystal core (PC-PCF). The following equation (Ali et al., 2022) can be used to determine this crucial feature:

$$\acute{\eta} = \frac{\int_x S_z dA}{\int_{all} S_z dA} \times 100 \qquad (5)$$

where S_z : z-component of the Pointing vector.

The denominator comprises the integration over all air holes and the TOPAS material, while the numerator only includes the integration over the air hole region, denoted as x, in order to assess the power fraction transferred through the air holes in the core. Terahertz light is confined within the core region, in the low-refractive-index air holes, allowing for a concentration of beam intensity within the core, as seen by a higher power percentage transmitted via the core's air holes. This suggests that the fiber may be used in medical equipment for single-mode terahertz imaging.

NORMALIZED FREQUENCY

The normalized frequency indicates the locations where polarization is necessary for the planned fiber to support a basic single mode. Because it reduces intermodal dispersion issues, single-mode propagation is essential for long-distance data transfer. To ensure single-mode operation, the V parameter, also known as the cutoff frequency equation, must not be more than 2.405 (Goto et al., 2004)

$$V = \frac{2\pi r f}{c} \sqrt{n_{co}^2 - n_{cl}^2} \qquad (6)$$

where r: radius of fiber core, c light speed in vacuum. n_{co} and n_{cl} : effective refractive index of the core and clad respectively.

BIREFRINGENCE

Birefringence (B) is defined as the real component of the disparity between the effective refractive indices of the x-polarized and y-polarized modes [25].

$$B = \left| n_{eff}^x - n_{eff}^y \right| \qquad (7)$$

n_{eff}^x and n_{eff}^y represent the effective refractive indices of the modes polarized along the x and y axes, respectively.

RESULTS AND DISCUSSION

SC-PCF PROPERTIES WITHOUT POROSITY

The confinement loss power fraction and dispersion of SC-PCF were investigated using three hexagonal layers of air holes without porosity inside the core. The effects of air hole widths between 200 and 240 µm were investigated with a 20 µm increment step. The pitch size and core diameter stay with out different at 300 µm and 350 µm, respectively. The calculation of the confinement loss for different air-hole diameters is shown in Figure 2. As the air hole width at 1THz increases, it decreases from 3.1782 × 10^{-5} dB/cm to 1.5263 × 10^{-9} dB/cm. With air hole diameters, a minimum confinement loss of 240 µm has been achieved. Consequently, the confinement loss is influenced by the air hole diameter.

Journal of Information Systems Engineering and Management
2025, 10(47s)
e-ISSN: 2468-4376
https://www.jisem-journal.com/

Research Article

The power ratio is displayed against frequency for 200 µm, 220 µm, and 240 µm air hole sizes in Figure 3. In contrast to the power that passes through the core when the diameter is 200 µm and 220 µm, or 56% and 61%, respectively, 65% of light passes through the fiber's core when the diameter is 240 µm, albeit some power passes through the cladding as losses at 1 THz. Additionally, the dispersion is plotted in Figure 4 and examined for various air hole diameters ranging from 200 µm to 240 µm. At every operating frequency range, the dispersion is negative. Furthermore, at lower working frequencies, the dispersion gets more negative as the width of the air holes increases. The dispersion increases to -52.85 Ps/THz/cm at 1 THz from -38.24 Ps/nm•km. Thus, it can be concluded that the radius of air holes has a significant impact on the dispersion. The effects of porosity in the core on the optical properties of the fiber are now being studied using an air hole with a diameter of 240 µm, which corresponds to the minimum value of confinement loss.

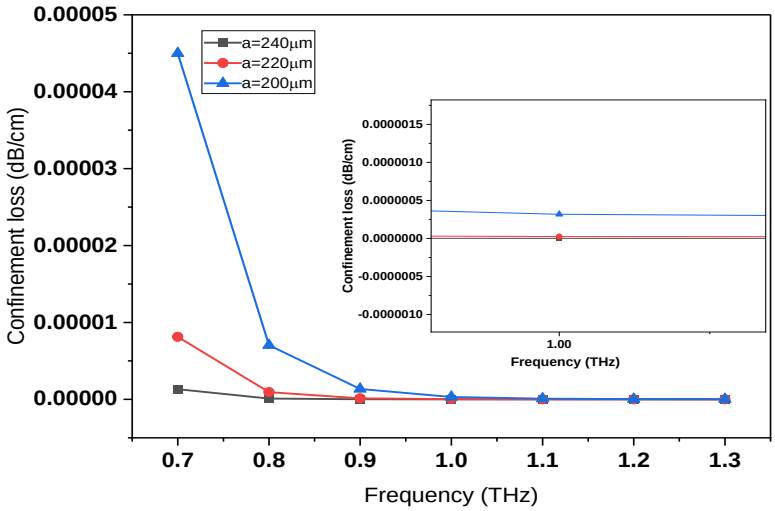

Figure 2. Illustrates the relationship between confinement loss and frequency.

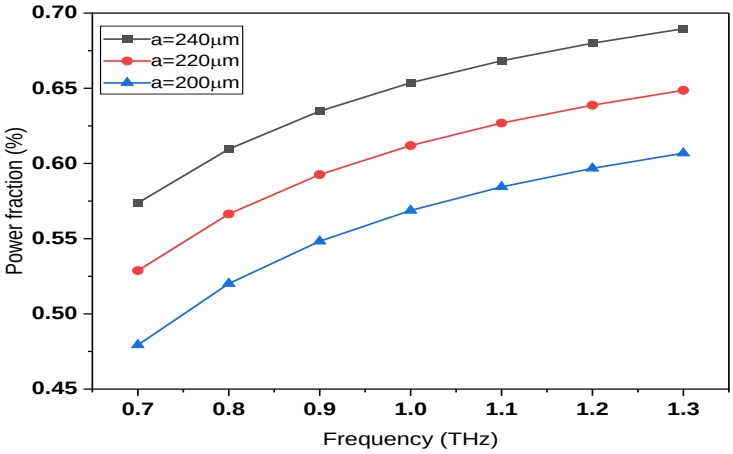

Figure 3 Illustrates the correlation between the power ratio and frequency.

Journal of Information Systems Engineering and Management
2025, 10(47s)
e-ISSN: 2468-4376
https://www.jisem-journal.com/

Research Article

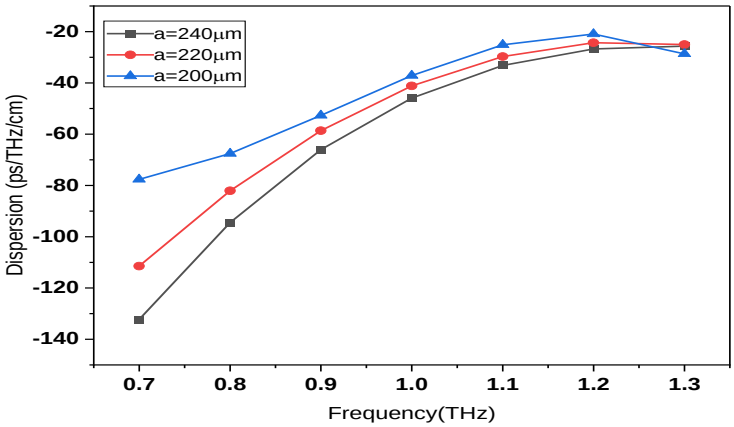

Figure 4. Depicts the correlation between dispersion and frequency.

EFFECTS THE SQUARE POROSITY ON THE PROPERTIES OF SC-PCFS

After optimizing the confinement loss, and the dispersion with 240 μm of air hole diameter, the square shaped porose are inserted inside the core. The core with these porosity called as defected core. Different diameter of square shaped poros (7%,16% and 28%) are used to improve the optical properties of the SC-PCFs. Now, the diameters of core and air hole are fixed at 300 μm and 240 μm respectively. The SC-PCF field is displayed in Figure 5 after two tiny square porosities are introduced into the core at 1 THz. The field is contained within the core's center, as seen in Figure 5. Therefore, it can be demonstrated that the presence of tiny square porosity in the core enhances the amount of light confinement within the PCF center.

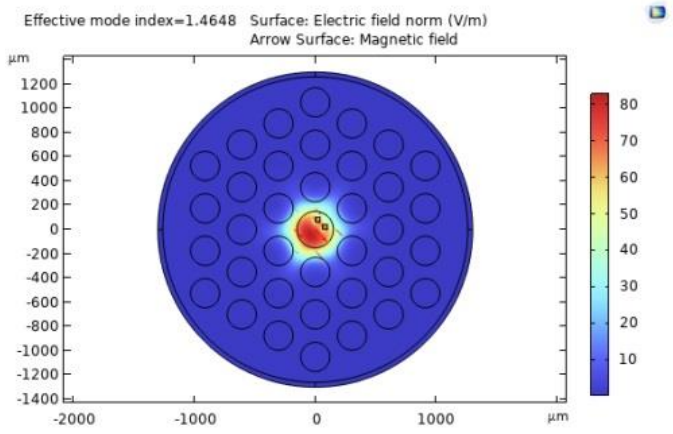

Figure 5: Cross sectional sectional and the filed of the SC-PCF at 1THz

The response of confinement loss as a function of the frequency for different porosity sizes is depicted in the Figure 6. From this Figure, it can be noticed that the confinement loss rapidly falls when the frequency is increased, this is due to increase the confined light in the core region when the frequency is increased which consequently is decrease the confinement loss. Further, the confinement loss incresed with the increasing the size of porosity at a fixed frequency, this is due to propagate more light through the porosity in the core rather than through the material.The low confinement loss of 1.39×10^{-5} cm^{-1} is found with 28%porosity at 1 THz.

Journal of Information Systems Engineering and Management
2025, 10(47s)
e-ISSN: 2468-4376
https://www.jisem-journal.com/

Research Article

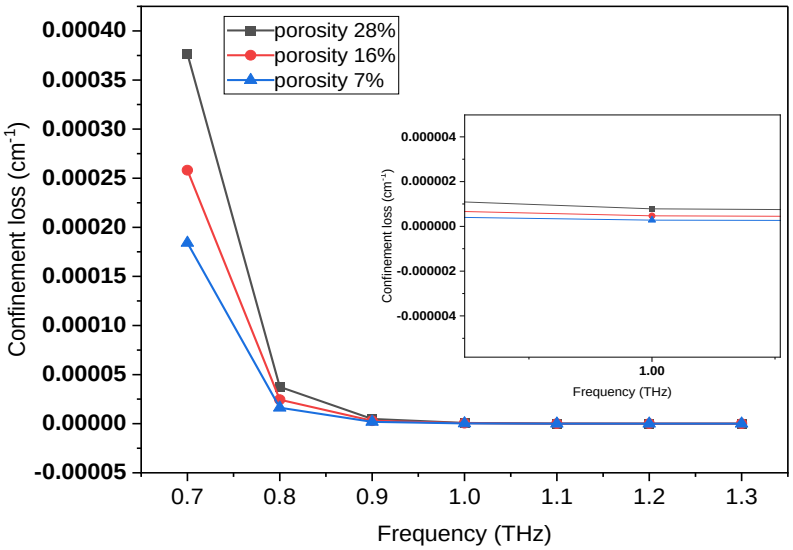

Figure 6. Illustrates confinement loss as function of the frequency for different shaped square porosity (7%, 16% and 28%)

Figure 7, illustrates the mode power fraction depends on the frequency in terahertzes range for different size of porosity. The mode power fraction is increase with increasing the frequency. Also, when the size porosity increases the core power fraction is decreased, which matches to the result of the confinement loss (see Figure 6). Further, the mode power fraction is remain constant for range of frequency from 1.1 to 1.3 THz, which is good for broadband THz transmission. At frequance of 1 THz, the power fraction is found to be 59%, 56% and 52% with porosity of 7% and 16 % and 28% respectively. The power fraction in core with 28% porosity is lower than the porosity of 7% and 16 %. This is due to absorption loss of the passing light in the square air porosity.

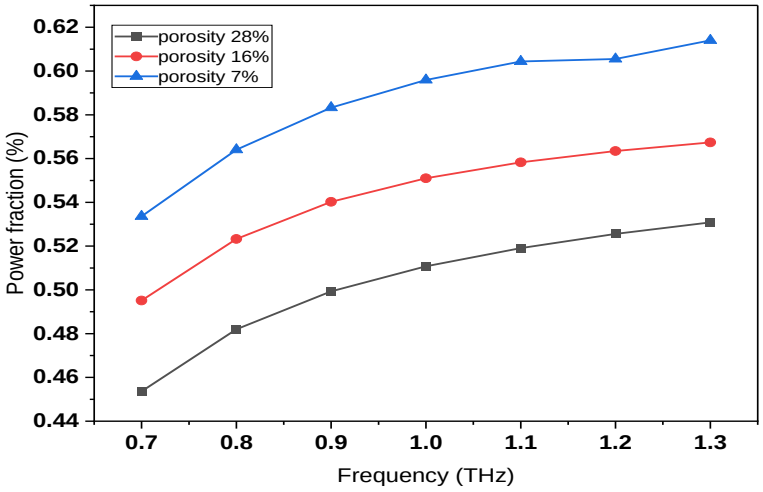

Figure 7. Illustrates the power fraction in core air hole as function of the frequency for different shaped square porosity (7%, 16% and 28%)

The response of V parameter as function of the THz frequency range for the suggested SC-PCFs with different size of porosity is shown in Figure 8. However, there are two types of the V parameter, when the V ≤ 2.405, the fiber will be as single mode fiber, and when the value of V > 2.405, the fiber will performance as a multimode fiber. as can be seen from Figure 8, the V-parameter for all porosity sizs is increased with increasing the frequency. Additionally, the V-parameter values are smaller than 2.405 which can be used the proposed SC-PCFs as a single mode fiber for long distance in communication system.

Journal of Information Systems Engineering and Management
2025, 10(47s)
e-ISSN: 2468-4376
https://www.jisem-journal.com/

Research Article

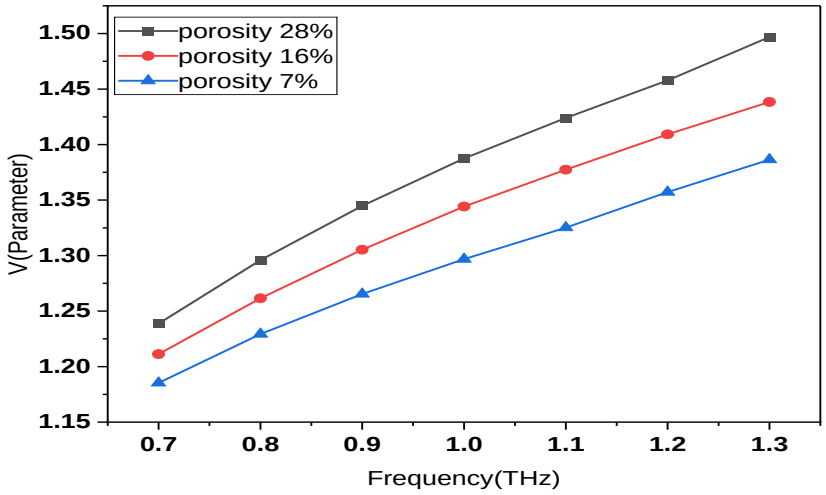

Figure 8: V parameter response versus THz frequency for different Porosities size

Figure 9 shows the birefringence versus the frequency of the suggested PC-PCFs for different porosity size (7%,16% and 28%) at diameter of core and air hole of 300 µm and 240 µm. As this Figure shows, the birefringence is increase when the size of porosity is increased.

The birefringence is high at lower values of the frequency and then its value start to decrease when the frequency range is increased. Additionally, the birefringence found to be larger when the core porosity is raised. It has been found that the birefringence value of 8.0×10^{-4} is achieved and presents a flat trend over the frequency ranging from 0.7–1.0 THz with 16% porosity. This is due to increase the area of the square air holes in the core. Consequently, the asymmetry of the porous in the core is become stronger and is lead to improvement of birefringence. This is important for the suggested PC-PCF to obtain a nearly constant birefringence with wide frequency range which can be used to control the chromatic dispersion for ultrafast pulse propagation.

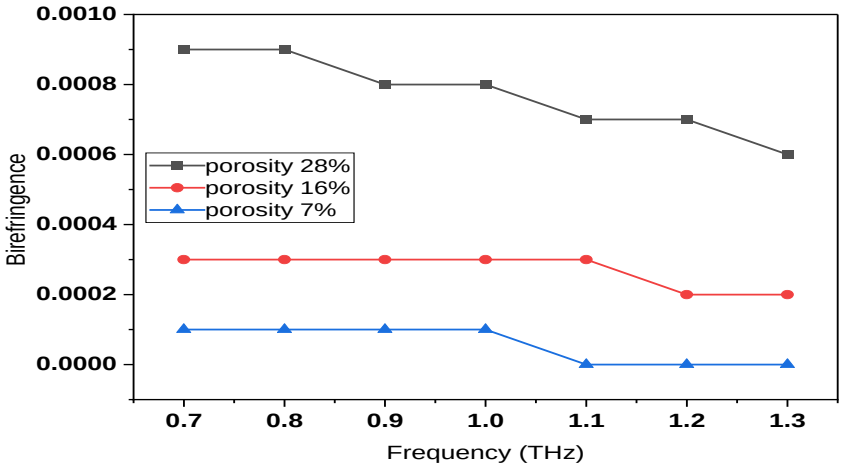

Figure 9. illustrates Birefringence as function of the frequency for different shaped square porosity (7%, 16% and 28%)

The dispersion vs frequency for variously shaped square porosity is shown in Figure 10. When the porosity is raised from 7% to 28% at 1 THz, it is evident that the dispersion turns negative. Additionally, by increasing the porosity in the core, the dispersion flattens at high operating frequencies. In comparison to the others, Figure 10 demonstrates that the dispersion is flatter with 28% porosity.

Journal of Information Systems Engineering and Management
2025, 10(47s)
e-ISSN: 2468-4376
https://www.jisem-journal.com/

Research Article

With a dispersion of β_2 = -42.303 ps/THz/cm, the flattened dispersion has been obtained throughout a broad frequency spectrum from 0.8 THz to 1.2 THz. By creating tiny holes in the core, the SC-PCF's dispersion is now enhanced. It is possible to illustrate a low dispersion that enhances broadband terahertz transmission across extended distances.

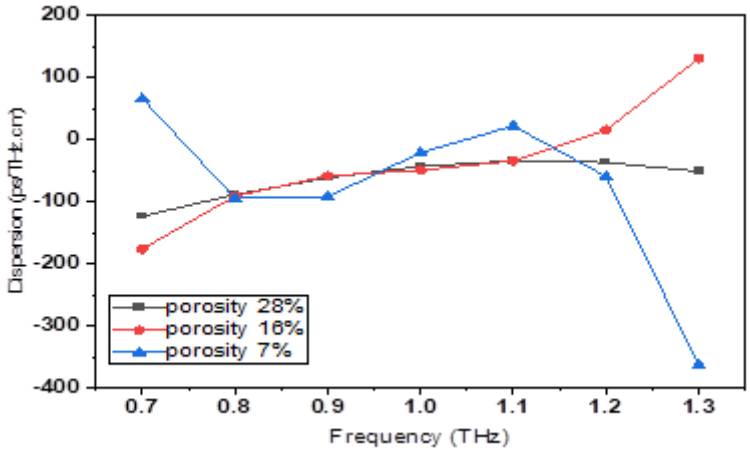

Figure 10. illustrates dispersion as function of the frequency for different shaped square porosity (7%, 16% and 28%)

IMPACT THE CIRCULAR POROSITY ON THE SC-PCF PROPERTIES

SC-PCF have a 300 µm core and 240 µm air hole diameter were chosen as the ideal settings in this section in order to investigate how circuler porosity affects the SC-PCF's characteristics. The aforementioned result indicates that the SC-PCF design which have 240µm diameter air holes was chosen because of its low confinement loss and low dispersion. This paper's primary objective is to improve terahertz radiation propagation and optimize optical characteristics by introducing tiny air holes into the fiber's core. Two circulator air-holes with varying diameters (d=20,30 and 40 µm) which they have been put in the core as porosities in order to carry out an optimum set of design SC-PCF. When the two tiny air holes are inserted as porosity inside the core at 1 THz, the cross section and field of the SC-PCF are displayed in Figure 11., 20 µm, 30 µm, and 40 µm are the chosen diameters of the tiny air holes, resulting in 7%, 16%, and 28% porosity in the core, respectively. Figure 11 shows that the field is contained within the core's center. Therefore, it can be demonstrated that the presence of tiny air holes in the core enhances the amount of light that is contained within the PCF center.

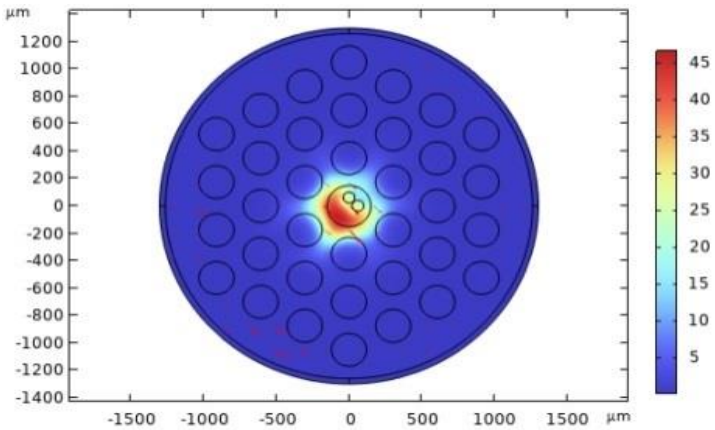

Figure 11. The field of the SC-PCF at 1THz

Journal of Information Systems Engineering and Management
2025, 10(47s)
e-ISSN: 2468-4376
https://www.jisem-journal.com/

Research Article

Figure 12 illistray the confinement loss of the planned SC-PCF as a function of frequency for various porosity sizes. It is evident that as the frequency increases, the confinement loss decreases. However, when the porosity in the core increases, so does the confinement loss.

In addition, the confinement loss of circule porosity is less than the confinement loss of the square porosity. It can be explained that the most of light propagates through the porous area, and as we know that circule area is less than the square area, as a result, less mode power of the circule porosity is leak out to the cladding compared to leak modes of the square porosity and confinement loss is decrease. With 28% porosity, the confinement loss is found to be 8.0441 × 10^{-8} dB/cm at 1 THz wich is decreased compared to confinement loss of the square porosity.

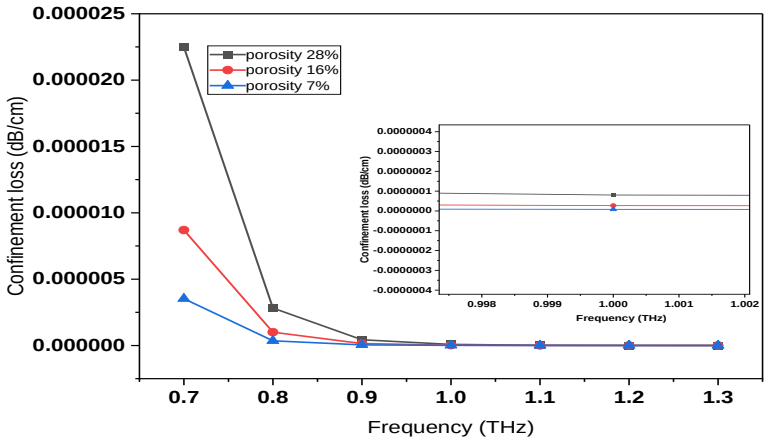

Figure:12. depicts the correlation between confinement loss and frequency for various porosity in the core.

For porosities of 7%, 16%, and 28%, Figure 13 displays the power fraction inside the core as a function of frequency in the terahertz range. As this figure illustrates, the power fraction is increase in the core region when the frequency is increased. Further, the power fraction is increase with increasing size of porosity at fixed frequency. Here we can observe that the power fraction with circuler porosity is largre than the power fraction with square porosity.With porosity of 28%, the power fraction of 51% is achieved in the core at 1THz. By reducing confinement loss, it has been discovered that the power fraction stays constant throughout a larger frequency range of 1 to 1.2 THz, which is crucial for broadband THz transmission.

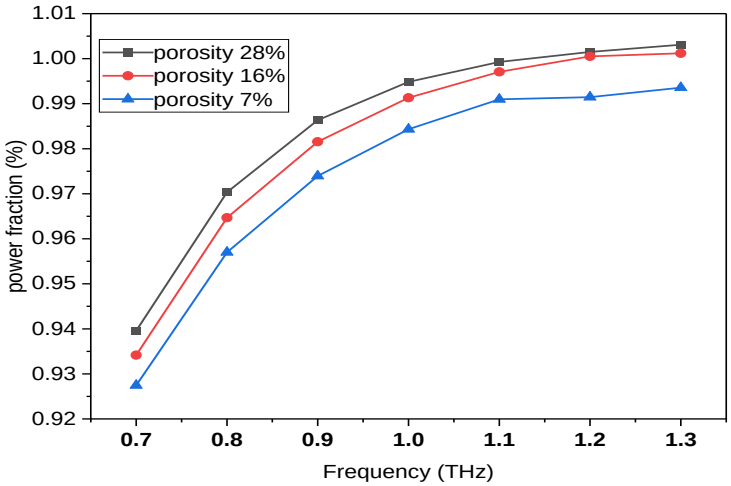

Figure:13. illustrates the relationship between power ratio and the frequency

Journal of Information Systems Engineering and Management
2025, 10(47s)
e-ISSN: 2468-4376
https://www.jisem-journal.com/

Research Article

The response of V parameter as function of the THz frequency range for the suggested SC-PCFs with different size of circule porosity is shown in Figure 14. From Figure 14, it is clear that with the increase in the value of frecuancy the V parameter value is increased. Additionally, the value of V parameter is increase with the increas in the size of porosity. Nonetheless, over the range of frequancy, the value of V still smaller than 2.405. hence, the proposed SC-PCFs can be used them as a single mode fiber for long distance in communication system.

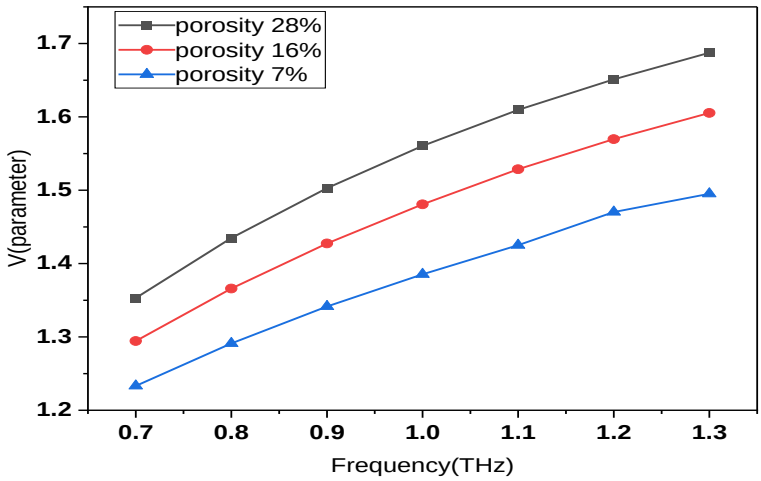

Figure 14: V parameter response versus THzfrequency for different size of the square porosity

Figure 15 shows the birefringence as a function of the frequency for different size of **circule** porosity (7%,16% and 28%). As this Figure shows, the birefringence is decrease when the frequency is increased. The birefringence is high at lower values of the frequency and then its value starts to decrease when the frequency range is increased. Additionally, the birefringence found to be larger when the core porosity is raised. Further, the birefringence value of 3.7×10^{-3} with 28% porosity is achieved over the frequency 1 THz. This is very important feature of the suggested PC-PCF for obtaining a nearly constant birefringence with wide frequency range.

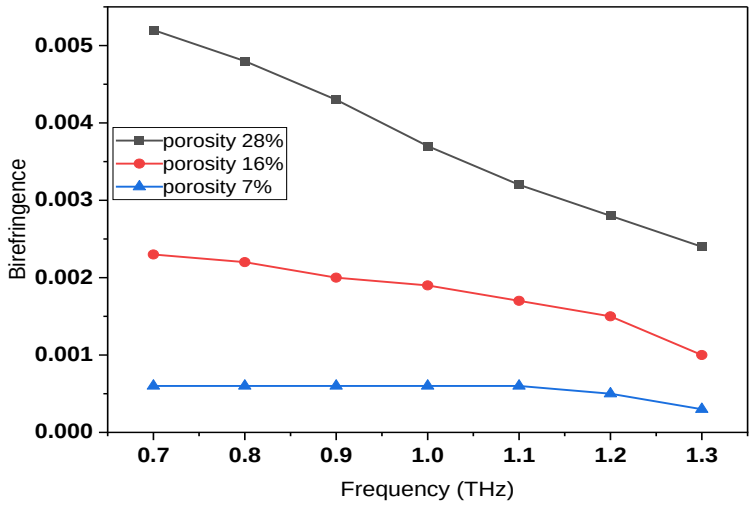

Figure 15. Birefringence as function of the frequency of the proposed SC-PCF with different circule porosity 7%, 16%, and 28% at Dcore=300µm

Journal of Information Systems Engineering and Management
2025, 10(47s)
e-ISSN: 2468-4376
https://www.jisem-journal.com/

Research Article

The THz frequency dependencies of the dispersion for different size of circule porosity have been depicted in Figure 16. It can be seen from this Figure the fiber is negative dispersive for all size of porosity. The negative dispersion is decrease and shifted near from the zero point when the porosity size is increased. Furthermore, flattened dispersion is the result of increasing the porosity in the core. The dispersion is flatter at 28% porosity compared to other porosities, as seen in Figure 16. For 28% porosity, the flattened dispersion with a dispersion of β2 = -43.2958 ps/THz/cm has been accomplished throughout a broad frequency bandwidth from 0.8 THz to 1.2 THz. The SC-PCF's dispersion is now improved by the little air holes in the middle. Long-distance broadband terahertz transmission is enhanced by its extremely low dispersion.

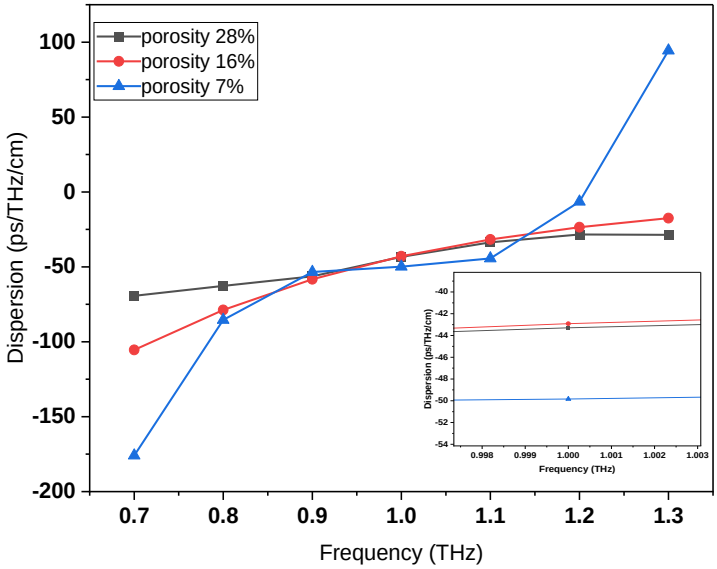

Figure 16. dispersion versus frequency of the proposed SC-PCF with different porosity 7%, 16%, and 28% at Dcore=300µm

CONCLUSION

The aim of this work is to achieve large birefringence and small/flatted dispersion by designed and examined the optical properties of hexagonal lattice SC-PCF. The optical properties of the proposed SC-PCF have been numerically investigated using COMSOL multiphysics 6.1 which based on the finite element method. It consists of a square air-hole porous core to drive high-refractive irefringence and a hexagonal lattice circular air-hole shell to enhance the confinement of the guided mode. Several physical features, such as varying core porosity and core diameter values at THz-range frequencies, define its guiding characteristics. It is possible to simultaneously produce an ultra-low flat dispersion of −0.01 ± 0.02 ps/THz/cm and a birefringence more than 7.1×10^{-2} in the broad frequency range of 0.7–1.3 THz. Other favorable characteristics of the suggested fiber include ultra-low confinement loss (about 7.08×10^{-12} cm^{-1}), high power-to-core ratio (around 52%), and good mode confinment because of low EML (<0.2 cm^{-1}). The suggested THz-PCF's superior steering capabilities can make it ideal for a variety of applications, including effective THz transmission, THz sensing, and other optical system designs.

ACKNOWLEDGMENTS

The authors would like to thank the professors (Mr. Faris M. Alhamadany, Msc. Phys., University of Newcastle, U.K., "Work in Nineveh Medicine College" and Mr. Alaa Mohammad (New York Times journal correspondent), who helped us rephrase the sentences grammatically and scientifically to suit what is presented in your journal.

Journal of Information Systems Engineering and Management
2025, 10(47s)
e-ISSN: 2468-4376
https://www.jisem-journal.com/

Research Article

REFERENCES

[1] Ali, A. M. , Alsaqa, R. & Sultan, N. S. (2022). Study of Thermodynamic Properties of Monoclinic Sulfur (Sβ) Under High Pressure Using Three Different Equations of State for the Treatment Scabies in Dermatology . International Journal of Thermodynamics , 25 (2) , 33-38 . doi: 10.5541/ijot.1003950.

[2] Aljunid. S.A., Islam R., Ahmed N., Ali S., Rana S., (2016). "Ultra-high birefringent and dispersion-flattened low-loss single-mode terahertz wave guiding," IET Communications, vol. 10, no. 13, doi:10.1049/iet-com.2015.0629

[3] Alobaidy M.R.A., Younus M.H., (2025). "Theoretical modeling and analysis of flatted dispersion pores in photonic crystal fiber core," Journal of Optics, doi:10.1007/s12596-025-02663-1

[4] Al-Saqa R.H., Jassim I.K., Uonis M.M., (2023). "Effect of KCl on the optical and structural properties of $CaZnO_3$ perovskite thin films," Ochrona przed Korozją, vol. 8, doi: 10.15199/40.2023.8.3

[5] Bowden B., Harrington J.A., Mitrofanov O., (2007). "Silver/polystyrene coated hollow glass waveguides for the transmission of terahertz radiation," Optics Letters, vol. 32, no. 20, doi:10.1364/OL.32.002945

[6] Brückner V., (2011). "To the use of Sellmeier formula," Senior Experten Service (SES) Bonn and HfT Leipzig, Germany, vol. 42.

[7] Chen L.J., Chen H., Kao T., Lu J., Sun C., (2006). "Low loss subwavelength plastic fiber for terahertz wave guiding," Optics Letters, vol. 31, no. 3, doi:10.1364/OL.31.000308

[8] Chen N., Liang J., Ren L., (2013). "High-birefringence, low-loss porous fiber for single-mode terahertz-wave guidance," Applied Optics, vol. 52, no. 22, doi:10.1364/AO.52.005297

[9] Chen Q, Jiang Z.P,. Xu G.X., . Zhang X.C, (2000). "Near-field terahertz imaging with a dynamic aperture," Optics Letters, vol. 25, no. 15, doi:10.1364/OL.25.001122

[10] Chou Chau Y.F., Lim C.M., Yoong V.N., Syafi'ie Idris M.N., (2015). "A simple structure of all circular-air-holes photonic crystal fiber for achieving high birefringence and low confinement loss," Journal of Applied Physics, vol. 118, no. 24, doi:10.1063/1.4938152

[11] Chowdhury S., Sen S., Ahmed K., Paul B.K., Miah M.B.A., Asaduzzaman S., (2017). "Porous shaped photonic crystal fiber with strong confinement field in sensing applications: design and analysis," Sensing and Bio-Sensing Research, vol. 13, doi:10.1016/j.sbsr.2017.03.002

[12] Gallozzi S., Scardia M., Maris M., (2020). "Concerns about ground-based astronomical observations: a step to safeguard the astronomical sky," arXiv preprint, doi:10.48550/arXiv.2001.10952

[13] Goto M., Quema A., Takahashi H., Ono S., Sarukura N., (2004). "Teflon photonic crystal fiber as terahertz waveguide," Japanese Journal of Applied Physics, vol. 43, no. 2B, doi:10.1143/JJAP.43.L317

[14] Haque M.M., Rahman M.S., Habib M.S., (2015). "A single mode hybrid cladding circular photonic crystal fiber for dispersion compensation and sensing applications," Photonics and Nanostructures-Fundamentals and Applications, vol. 14, doi:10.1016/j.photonics.2015.01.006

[15] Hasan M.R., Anower M.S., Islam M.A., Razzak S.M.A., (2016). "Polarization-maintaining low-loss porous-core spiral photonic crystal fiber for terahertz wave guidance," Applied Optics, vol. 55, no. 15, doi:10.1364/AO.55.004145

[16] Hossain A., Namihira Y., (2014). "Light source design using Kagome lattice hollow core photonic crystal fibers," Optical Review, vol. 21, no. 4, doi:10.1007/s10043-014-0076-z

[17] Islam M.R., Kabir M.F., Talha K.M.A., Arefin M.S., (2020). "Highly birefringent honeycomb cladding terahertz fiber for polarization-maintaining applications," Optical Engineering, vol. 59, no. 1, doi:10.1117/1.OE.59.1.016113

[18] Islam R., Habib M.S., Hasanuzzaman G.K.M., Rana S., Sadath M., (2016). "A novel porous fiber based on dual-asymmetry for low-loss polarization maintaining THz wave guidance," Optics Express, vol. 41, no. 3, doi:10.1364/OL.41.000440

[19] Li X.H., Wang Y.S., Zhao W., Liu X., Wang Y., Tsang Y.H., (2012). "All-fiber dissipative solitons evolution in a compact passively Yb-doped mode-locked fiber laser," Journal of Lightwave Technology, vol. 30, no. 15, doi:10.1109/JLT.2012.2201210

Research Article

[20] Liu H.B., Zhong H., Karpowicz N., Chen Y., Zhang X.C., (2007). "Terahertz spectroscopy and imaging for defense and security applications," Proceedings of the IEEE, vol. 95, no. 8,. doi:10.1109/JPROC.2007.898903
[21] Nagatsuma T., Ducournau G., Renaud C.C., (2016). "Advances in terahertz communications accelerated by photonics," Nature Photonics, vol. 10, no. 6, doi:10.1038/nphoton.2016.65
[22] Paul B.K., Ahmed K., (2019). "Highly birefringent TOPAS-based single-mode photonic crystal fiber with ultra-low material loss for terahertz applications," Optical Fiber Technology, vol. 53, doi:10.1016/j.yofte.2019.102031
[23] Pawar A.Y., Sonawane D.D., Erande K.B., Derle D.V., (2013). "Terahertz technology and its applications," Drug Invention Today, vol. 5, no. 2, doi:10.1016/j.dit.2013.03.009
[24] Rabih L., Ali G.G., Younus M.H., (2201). "Evaluation of optical and electrical properties of TiO_2 thin films doped with Cu ions," AIP Conference Proceedings, vol., no. 1, 2019. doi:10.1063/1.5141425
[25] Skorobogatiy M., Dupuis A., (2007). "Ferroelectric all-polymer hollow Bragg fibers for terahertz guidance," Applied Physics Letters, vol. 90, no. 11, doi:10.1063/1.2713137
[26] Sultana J., Islam M.S., Faisal M., Islam M.R., Ng B.W.H., (2018). H. Ebendorff-Heidepriem, D. Abbott, "Highly birefringent elliptical core photonic crystal fiber for terahertz application," Optics Communications, vol. 407, doi:10.1016/j.optcom.2017.09.020
[27] Wang K., Mittleman D.M., (2004). "Metal wires for terahertz waveguiding," Nature, vol. 432, no. 7015, doi:10.1038/nature03040
[28] Xu W.X., Guo P.L., Li X.H., Hui Z.Q., Wang Y., Shi Z., (2020). "Sheet-structured bismuthene for near-infrared dual-wavelength harmonic mode-locking," Nanotechnology, vol. 31, no. 22, doi:10.1088/1361-6528/ab7674
[29] Younus M.H., Ali G.G., Salih H.A., (2021). "The reinforced optical fiber sensing with bilayer AuNPs/SiC for pressure measurement: characterization and optimization," Journal of Physics: Conference Series, vol. 1795, no. 1,. doi:10.1088/1742-6596/1795/1/012002
[30] Younus M.H., Ameen O.F., Ibrahim R.K.R., Redzuan N., (2017). "Fuel detection system using OTDR with multimode fiber," Jurnal Teknologi (Sciences & Engineering), vol. 79, no. 3, doi:10.11113/jt.v79.768
[31] Yu C., Fan S., Sun Y., Pickwell-MacPherson E., (2012). "The potential of terahertz imaging for cancer diagnosis: a review of investigations to date," Quantitative Imaging in Medicine and Surgery, vol. 2, no. 1 doi:10.3978/j.issn.2223-4292.2012.01.04
[32] Zaytsev K.I., Kudrin K.G., Karasik V.E., Reshetov I.V., Yurchenko S.O., (2015). "In vivo terahertz spectroscopy of pigmentary skin nevi: pilot study of non-invasive early diagnosis of dysplasia," Applied Physics Letters, vol. 106, no. 5, doi:10.1063/1.4907350
[33] Zhang B., Rahmatullah B., Wang S.L., Zaidan A.A., Zaidan B.B., Liu P., (2023). "A review of research on medical image confidentiality related technology coherent taxonomy, motivations, open challenges and recommendations," Multimedia Tools and Applications, vol. 82, no. 1, doi:10.1007/s11042-020-09629-4
[34] Zhao G., Mors M.T., Wenckebach T., (2002). "Terahertz dielectric properties of polystyrene foam," Journal of the Optical Society of America B, vol. 19, no. 6, doi:10.1364/JOSAB.19.001476